Agriculture and Food

AIMS Agriculture and Food, 11(1): 95–117.
DOI: 10.3934/agrfood.2026006
Received: 22 July 2025
Revised: 01 February 2026
Accepted: 14 February 2026
Published: 10 March 2026

https://www.aimspress.com/journal/agriculture

Research article

Antioxidant and antifungal activities of green synthesized silver nanoparticles in comparison with essential oil, and extracts of *O. vulgare* leaves

Latifeh Pourakbar[1,*], Neda Farnad[1], Sina Siavash Moghaddam[2], Jelena Popović-Djordjević[3] and Angelo Maria Giuffrè[4,*]

[1] Department of Biology, Faculty of Science, Urmia University, Urmia, Iran
[2] Department of Plant Production and Genetics, Faculty of Agricultural Sciences, University of Guilan, Rasht, Iran
[3] University of Belgrade, Faculty of Agriculture, Department of Food Technology and Biochemistry, Belgrade, Serbia
[4] Department AGRARIA, University of Studies "*Mediterranea*" of Reggio Calabria, 89124, Reggio Calabria, Italy

* **Correspondence:** Email: amgiuffre@unirc.it, Tel: +393277022840; la.pourakbar@urmia.ac.ir.

Abstract: Aromatic plant essential oils (EO) and their derivatives are promising, eco-friendly alternatives for fungal disease management in plants due to their low toxicity and environmental compatibility. However, practical applications are often limited by challenges such as high volatility, poor water solubility, and inefficient dispersion. To address these limitations, we developed an innovative approach to enhance the stability and antimicrobial efficacy of *Origanum vulgare* extracts through the green synthesis of silver nanoparticles (AgNPs). The synthesized AgNPs were characterized using UV-Vis spectroscopy and scanning electron microscopy (SEM). UV-Vis analysis revealed characteristic surface plasmon resonance (SPR) peaks at 445 nm (aqueous AgNPs) and 435nm (methanolic AgNPs), confirming nanoparticle formation. The aqueous extract exhibited the highest total phenolic content (50.3 ± 1 mg gallic acid/g), while methanolic AgNPs demonstrated the strongest antioxidant activity, scavenging 89.7 ± 0.2% of DPPH radicals with an IC_{50} of 19.6 ± 0.3 µg/cm³. The antifungal activity of *O. vulgare* essential oil, AgNPs, and crude extracts was evaluated against *Aspergillus niger*, *Botrytis cinerea*, and *Penicillium expansum*. GC-MS analysis identified carvacrol (56.53%), thymol (21.18%), p-cymene (6.22%), and γ-terpinene (5.67%) as the major EO

constituents. We are the first to report the green synthesis of AgNPs using *O. vulgare* extracts with comparative evaluation against crude extracts and essential oils for enhanced antifungal application. This study presents a significant advancement in fungal control strategies by demonstrating that AgNPs synthesized from *O. vulgare* extracts not only retain the high antifungal and antioxidant properties of the essential oil but also overcome its limitations through improved stability, water solubility, and dispersion. The findings suggest that AgNPs synthesized from *O. vulgare* are a more effective and sustainable alternative to conventional essential oils for combating fungal pathogens in agricultural and post-harvest applications.

Keywords: AgNPs; antifungal activity; antioxidant activity; essential oil; green synthesis; *Oregano* leaves extract

1. Introduction

The adoption of green nanotechnology across industries has been rapid and widespread because it employs environmentally friendly, cost-effective, and non-toxic chemicals [1]. Among nanoparticles, AgNPs are widely recognized for their potent bioactive properties, including strong antioxidant, antimicrobial, antifungal, antifungal, and antiviral effects, as well as unique optical characteristics. Owing to these versatile properties, AgNPs have emerged as promising candidates for diverse applications in medical science, textiles, the food industry, optics, conductive materials, and environmental remediation [2]. AgNPs demonstrate strong potential as environmentally friendly fungicides for sustainable agriculture. They effectively inhibit the growth of plant pathogenic fungi such as *Fusarium* spp. and *Magnaporthe oryzae*, while being non-toxic to seeds. Their use offers a green alternative to conventional chemical fungicides, with the added benefit of synergistic effects when combined with antifungal agents, thereby enhancing efficacy and reducing the risk of resistance development [3,4]. Various physical, chemical, and biological methods have been developed for AgNPs synthesis. Notably, plant-mediated green synthesis has gained considerable attention due to its eco-friendly and sustainable approach. This method involves the reduction of Ag^+ ions using phytochemicals derived from plant extracts [5]. Plant secondary metabolites, particularly phenolic compounds such as flavonoids and phenolic acids, serve as key sources of phytochemicals with inherent antioxidant capabilities. These antioxidants play a critical role in human health by mitigating oxidative damage through the stabilization of free radicals and inhibition of free radical-mediated chain reactions in biological systems [6]. The extraction of phenolic compounds from plants is a critical initial step in evaluating their antioxidant potential. Among the extraction techniques available, solvent extraction remains the most widely used method for isolating natural bioactive compounds from medicinal plants. Solvent polarity plays a key role in this process, particularly when targeting polar solutes. Due to their high polarity, solvents such as methanol, ethanol, and water are highly effective in successfully extracting phenolic compounds from plant matrices [7]. *Origanum vulgare*, an aromatic plant belonging to the Lamiaceae family, is native to Mediterranean regions and Asia. Among the two predominant *Origanum* species (*O. vulgare* and *O. majorana*), *O. vulgare* is particularly significant in Iran, where it finds extensive applications in the food industry, traditional medicine, perfumery, and as a natural antimicrobial agent [8,9]. This antimicrobial potential is especially relevant given the substantial threat posed by fungal pathogens, which, unlike most benign fungal species, account for

approximately two-thirds of all infectious plant diseases and present significant risks to agricultural systems and human health. Consequently, plant-derived antifungal agents such as *O. vulgare* represent promising alternatives for sustainable disease management. Among these, three major necrotrophic fungi, *Aspergillus niger*, *Botrytis cinerea*, and *Penicillium expansum,* are responsible for widespread infections in vegetables, fruits, and crop plants, with some species also exhibiting zoonotic potential [10,11]. Conventional disease management has relied heavily on synthetic fungicides. However, growing concerns regarding their toxicity and environmental persistence have spurred interest in natural alternatives. This shift has driven increased research into plant-derived antimicrobial agents, including extracts, essential oils (EOs), and green-synthesized nanoparticles, for their potential applications in sustainable agriculture and medicine. Studies have demonstrated promising antifungal and antimicrobial properties in these natural compounds, highlighting their viability as eco-friendly alternatives to synthetic fungicides [12,13]. Despite their potent antifungal properties, plant EOs face several limitations, including high volatility, poor water solubility, susceptibility to oxidation, challenges in dispersion, and potential interactions with other compounds, which restrict their practical application in the biological control of insect pests [14]. Moreover, studies indicate that *Foeniculum vulgare* essential oil-enriched ZnO nanorods (ZnO-NRs) demonstrate synergistic antibacterial activity against opportunistic food (*Pseudomonas aeruginosa* and *Bacillus subtilis*) and plant pathogenic (*Pseudomonas syringae* pv. phaseolicola) bacterial disease agents [15]. Additionally, it is reported that the green synthesized ZnO-NPs play a key role against plant pathogenic bacterial disease agents [16].

This article comprises two major sections. In the first section, we focus on the simple, rapid, green, and cost-effective biosynthesis and characterization of silver nanoparticles (AgNPs) using methanolic and aqueous extracts of *O. vulgare* leaves. Plant extract-mediated synthesis offers a practical and scalable green chemistry approach that overcomes several limitations of essential oil-based methods, including volatility, poor aqueous solubility, and storage instability. The synthesized AgNPs were characterized using UV-Vis spectrophotometry and scanning electron microscopy (SEM). Additionally, the total phenolic content and antioxidant activities of the plant extracts and the resulting AgNPs were evaluated.

In the second section, we present a comparative analysis of the antifungal efficacy of *O. vulgare* essential oil (EO), crude plant extracts, and biosynthesized AgNPs. The bioactive constituents of the leaf essential oil were further characterized by gas chromatography–mass spectrometry (GC-MS) to identify the compounds contributing to its antimicrobial properties.

2. Materials and methods

2.1. Materials

2.1.1. Chemicals

1,1-Diphenyl-2-picrylhydrazyl (DPPH) and Tween-20 were obtained from Sigma-Aldrich Co. (Gillingham, UK). All other solvents and chemical reagents were of analytical grade and purchased from Merck KGaA (Darmstadt, Germany).

2.1.2. Plant materials

Fresh leaves of *O. vulgare* were collected during August 2020 from Shohada Valley (Urmia, West Azerbaijan Province, Iran). Botanical identification was authenticated by comparison with voucher specimens at the Herbarium of the Department of Biology, Faculty of Science, Urmia University, Iran.

2.2. Methods

2.2.1. Preparation of extracts and essential oil

Fresh leaves of *O. vulgare* were manually fragmented and shade-dried at ambient temperature (25 °C) before being ground to a fine powder. For solvent extraction, 10 g aliquots of dried material were separately extracted with 100 mL methanol using orbital agitation (150 rpm, 3 h, light-protected) and with 100 mL distilled water in a temperature-controlled water bath (80 °C, 15 min). Both extracts were filtered through Whatman No. 1 filter paper and concentrated under reduced pressure. Essential oils were obtained by hydrodistilling 50 g fresh material in a Clevenger apparatus for 3 h, with extraction yields calculated as (weight of extract/weight of input material) × 100. All solvents were analytical grade, with methanol from Sigma-Aldrich and equipment including MEMMERT water baths and Laborxing glassware. The extraction yield was calculated using the equation:

$$R\% = (m/M) * 100 \quad (1)$$

where m is the mass of the extracted oil (g) and M is the initial plant biomass (g). The extracts and EOs were stored at 4 °C in the dark until further evaluations.

2.2.2. Preparation of AgNPs

For nanoparticle synthesis, 1 mL of aqueous or methanolic extract was combined with 100 mL of 1 mM $AgNO_3$ solution and incubated at 80 °C for 5 min, followed by 24 h stabilization at room temperature [17]. Prior to SEM analysis, the products were filtered through 0.45 μm membranes, oven-dried at 70 °C for 12 h, and imaged using field-emission SEM (Fe-SEM, TESCAN MIRA II LMU).

2.2.3. Characterization techniques

UV-Vis spectral analysis was performed using a Biowave WPA spectrophotometer (UK) from 200–800 nm to characterize extracts and AgNPs. Nanoparticle stability was assessed through biweekly UV-Vis monitoring over two months. Morphological characterization was conducted via SEM.

2.2.4. Determination of total phenolic contents (TPC)

TPC was quantified using a modified Folin-Ciocalteu assay [18]. A total of 1 mL of Folin-Ciocalteu reagent and 10% (w/v) Na_2CO_3 were added to 0.01 mL samples, followed by 30 min dark incubation. Absorbance at 765 nm was measured, with TPC expressed as gallic acid equivalents (GAE)/g dry weight (calibration curve: $y = 0.042x - 0.023$, $R^2 = 0.998$).

2.2.5. Determination of DPPH radical scavenging activity

DPPH radical scavenging activity of plant extracts and AgNPs was evaluated by mixing 0.01 mL samples with 2 mL methanolic DPPH (0.004%) [19]. After 30 min dark incubation, absorbance at 520 nm was measured.

The DPPH radical scavenging activities were calculated according to the following formula:

$$\%\text{DPPH scavenging activity} = ((A_0 - A_1)/A_0) * 100 \quad (2)$$

where A_0 represents the absorbance of the control (containing only DPPH solution without *O. vulgare* extract or AgNPs), and A_1 denotes the absorbance following treatment with *O. vulgare* extract or AgNPs. The reduction in DPPH absorbance correlates directly with radical scavenging capacity. Results were quantified as the half-maximal inhibitory concentration (IC_{50}), which was determined by plotting scavenging percentage against sample concentration and calculating the concentration required for 50% radical neutralization.

2.2.6. Evaluation of antifungal activity

The antifungal activity was evaluated using the agar diffusion method with potato dextrose agar (PDA). PDA medium was prepared by suspending 39 g/L in distilled water, followed by autoclaving at 121 °C for 20 minutes. Serial concentrations of *O. vulgare* essential oil (200, 400, 600, 800, and 1000 μg/mL) were incorporated into the sterilized PDA medium, with 0.1% V/VTween-20 added as an emulsifier. Aliquots of 25 mL of the amended medium were aseptically dispensed into sterile Petri dishes (90 mm diameter), with oil-free PDA serving as the negative control. Fungal inocula (5–7 day-old cultures) were centrally placed on the prepared media and incubated at 25 ± 2 °C. Mycelial growth was monitored daily, with radial measurements taken when the control plates reached full colonization (edge of the dish). The experiment was conducted four times for each concentration. The percentage inhibition of mycelial growth (I%) was calculated using the formula:

$$I\% = [(Rc - Rt)/Rc] \times 100 \quad (3)$$

where:
Rc = Radial growth in control (mm);
Rt = Radial growth in treatment (mm) mg/L [20].

The antifungal activity of AgNPs and plant extracts was evaluated using the agar well diffusion method. Fungal cultures were first grown on PDA until sporulation occurred. A standardized inoculum was prepared by adjusting the spore suspension to 10^5 conidia/mL in sterile 0.85% saline solution. This suspension was uniformly spread on fresh PDA plates using a sterile spreader. Using an aseptic technique, 6-8 mm diameter wells were created in the inoculated agar with a sterile cork borer. AgNPs and extracts were introduced into the wells, with deionized water serving as the negative control. All plates were incubated in darkness at 25 ± 2 ℃ for 96 hours. Following incubation, the diameter of inhibition zones (including well diameter) was measured to the nearest millimeter using digital calipers. The experiment was performed in triplicate, with mean values reported for each treatment.

2.2.7. Gas chromatography-mass spectrometry (GC–MS) analysis

The chemical composition of the essential oil was analyzed using an Agilent 7890A gas chromatograph (Agilent Technologies, Palo Alto, CA, USA) equipped with an HP-5MS capillary column (30 m × 0.25 mm i.d., 0.25 μm film thickness; 5% phenyl methyl siloxane stationary phase). The GC system was coupled to a mass selective detector operating in electron impact ionization mode at 70 eV. The oven temperature program was initiated at 80 °C (held for 3 min), then ramped at 8 °C min^{-1} to 180 °C. The injector and interface temperatures were maintained at 250 °C and 220 °C, respectively. Helium carrier gas was used at a constant flow rate of 1.0 mL min^{-1}, with a 1 μL injection volume in split mode (split ratio 50:1). Mass spectra were acquired in scan mode (m/z 30–300) with an ion source temperature of 200 °C and electron multiplier voltage of 3000 V [21]. Compounds were identified using a dual-identification approach combining mass spectral matching and retention index (RI) verification.

2.2.8. Data analysis

All experimental data were analyzed using SPSS Statistics software (version 16.0, IBM Corp.). One-way analysis of variance (ANOVA) followed by Duncan's multiple range test was performed to determine significant differences among treatments at $p < 0.05$. Data visualization was conducted using Microsoft Excel (2016 version), with results expressed as mean ± standard deviation of triplicate measurements.

3. Results and discussion

3.1. Characterization techniques

Two distinct types of AgNPs, differing in color and size, were synthesized. The nanoparticles were characterized through three complementary techniques: visual color assessment, UV-Vis spectroscopy, and scanning electron microscopy (SEM). As shown in Figure 1, sample tubes contain *O. vulgare* extracts (a, b) and the resulting AgNPs solutions (e, f). Nanoparticle synthesis was achieved by reacting plant extracts with $AgNO_3$ in a rapid 5-minute process. The immediate color change observed, transitioning to various shades of brown, confirmed the bio-reduction of Ag^+ ions mediated by the plant extracts. Specifically, dark brown and grey-brown coloration developed in aqueous and methanolic AgNP suspensions, respectively. These color variations were attributable to differences in initial synthesis conditions, particularly the solvent system. Furthermore, AgNPs prepared using different solvents exhibited distinct morphologies and sizes [22], as confirmed by subsequent SEM analysis. The successful synthesis of AgNPs was verified through UV-Vis spectroscopy and SEM. UV-Vis spectroscopy represents a fundamental characterization technique for nanoparticle detection, relying on the distinctive surface plasmon resonance (SPR) exhibited by metallic nanoparticles. The SPR phenomenon typically produces characteristic absorption bands for AgNPs in the 320–520 nm range [23]. Notably, while the methanolic extract alone exhibited a weak absorption peak at approximately 670 nm, the aqueous extract of *O. vulgare* demonstrated no significant peaks across the 200–800 nm spectrum. Following nanoparticle synthesis, distinct SPR peaks emerged at 445 nm and 435 nm for AgNPs produced using aqueous and methanolic extracts, respectively. The observed peak broadening suggests potential nanoparticle aggregation (Figure 1A, B), a phenomenon commonly associated with interparticle interactions and size distribution effects.

The methanolic AgNPs exhibited a slight redshift in their UV-Vis absorption spectrum, which may be attributed to their reduced particle size. This observation is consistent with the well-established size-dependent plasmonic behavior of nanoparticles, where larger AgNPs typically demonstrate a more pronounced redshift in their absorption maximum [24].

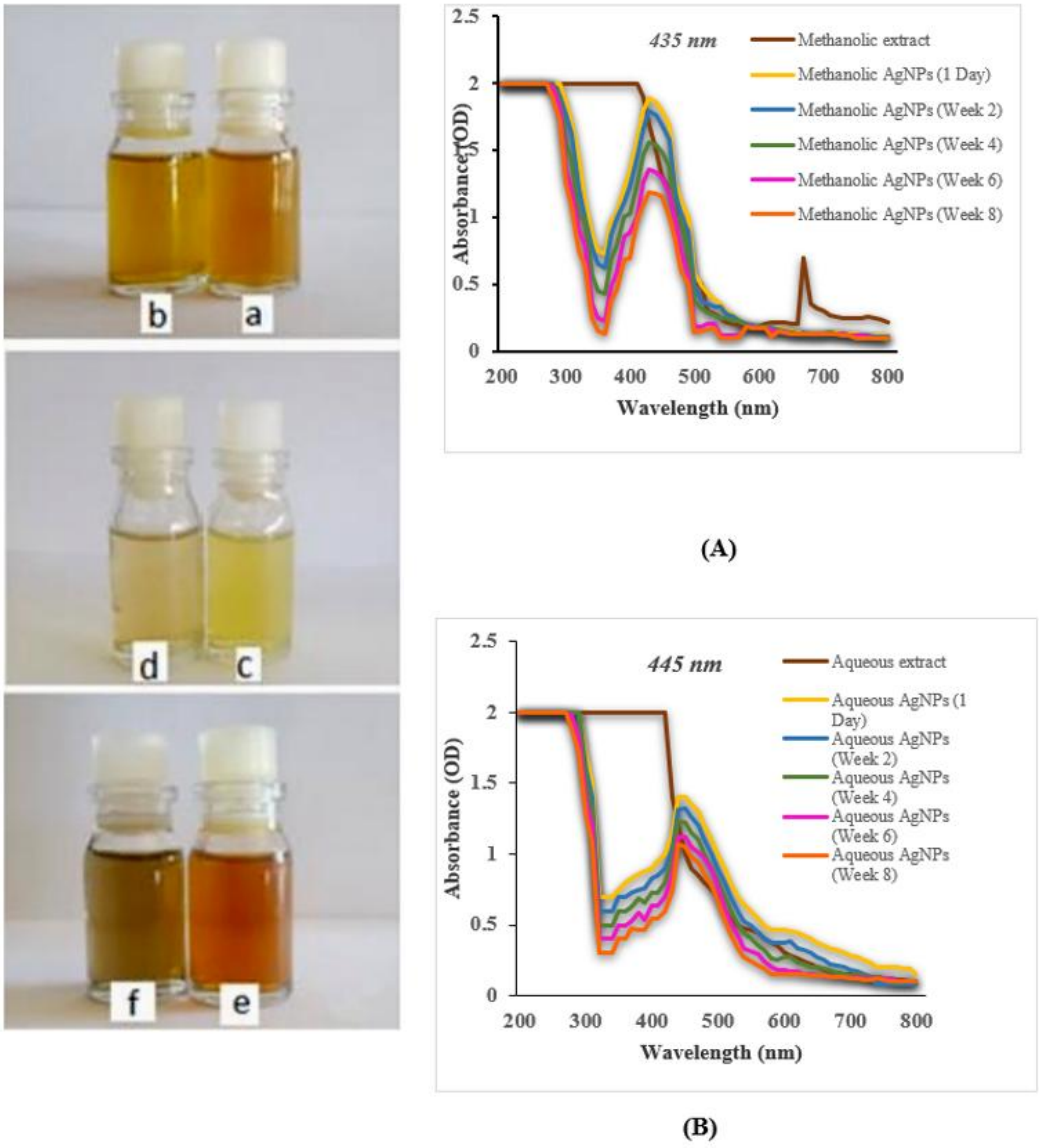

Figure 1. The UV-Vis absorption spectra tracked the green synthesis of AgNPs over 8 weeks, revealing distinct surface plasmon resonance peaks at 445 nm for AgNPs produced with aqueous extracts (A) and 435 nm for those synthesized using methanolic extracts (B). Accompanying visual changes included: (a) the aqueous extract, (b) the methanolic extract, (c) aqueous extract mixed with $AgNO_3$ at t = 0 min, (d) methanolic extract mixed with $AgNO_3$ at t = 0 min, (e) aqueous AgNPs after 1 day of reaction, and (f) methanolic AgNPs after 1 day of reaction, with color transitions indicating progressive nanoparticle formation.

Studies have demonstrated the successful biosynthesis of AgNPs using plant extracts as reducing agents. For instance, *Ceropegia thwaitesii* leaf extract has produced AgNPs averaging 100 nm in size,

exhibiting a characteristic SPR peak at 430 nm [25]. Similarly, *Thalictrum foliolosum* root extract has generated spherical AgNPs, as evidenced by a distinct SPR peak at 420 nm in UV-Vis spectra [26]. In this study, the synthesized AgNP solutions demonstrated exceptional stability, maintaining their colloidal properties without visible precipitation or significant alterations in color and absorbance patterns over a two-month observation period. This stability suggests effective capping of the nanoparticles by phytochemical constituents present in the plant extracts, which prevent aggregation and preserve the nanoparticles' optical properties.

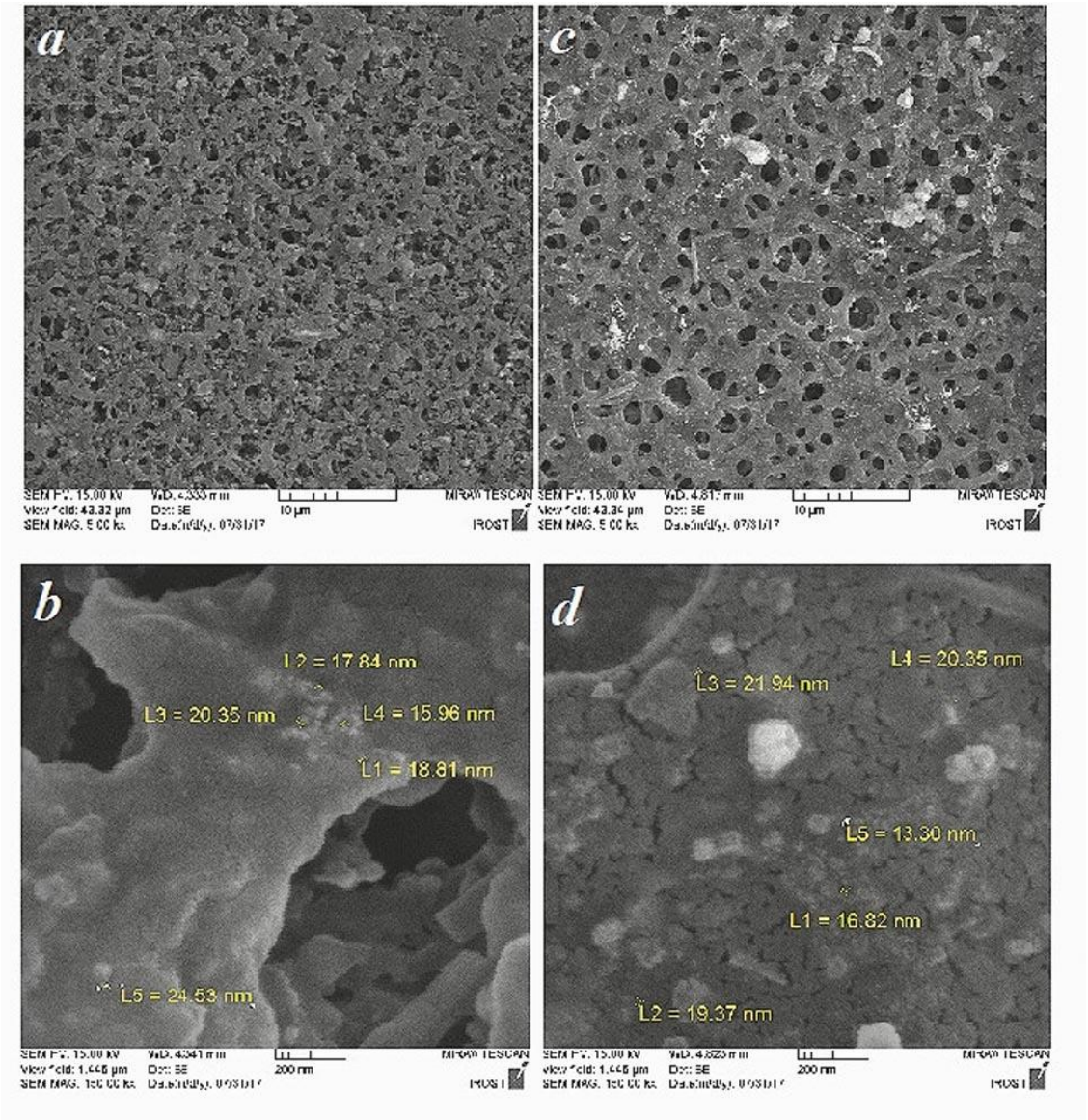

Figure 2. Scanning electron micrographs of biosynthesized AgNPs using *O. vulgare* extracts: (a,b) AgNPs synthesized with aqueous extract showing particle sizes of 19.43 nm; (c,d) AgNPs produced with methanolic extract demonstrating reduced particle sizes (18.35 nm) and improved dispersion. Scale bars: 200 nm. The micrographs reveal spherical morphology with aqueous-derived AgNPs exhibiting greater aggregation tendency compared to methanol-synthesized counterparts, correlating with UV-Vis spectral observations.

SEM analysis was employed to characterize the size and morphology of the synthesized silver nanoparticles. While SEM typically provides micron-scale resolution, our high-resolution field-emission SEM enabled precise nanoparticle characterization at the nanoscale. Comparative analysis revealed that AgNPs synthesized using methanolic extract exhibited reduced particle sizes compared to those produced with aqueous extract (Figure 2). The SEM micrographs demonstrated that aqueous and methanolic extracts of *O. vulgare* yielded predominantly spherical AgNPs with diameters ranging from 13–24 nm. Quantitative analysis showed mean particle sizes of 19.43 nm (aqueous extract) and 18.35 nm (methanolic extract). These findings correlated with the observed red-shift in UV-Vis spectra, confirming the relationship between particle size and optical properties.

3.2. Total phenolic contents (TPC)

The antioxidant capacity of plant extracts is fundamentally governed by the structural features of phenolic compounds. These phytochemicals, encompassing simple phenols and polyphenols such as flavonoids, possess hydroxyl groups attached to aromatic benzene rings. This characteristic molecular configuration enables phenolic compounds to serve as effective hydrogen donors and free radical scavengers, thereby terminating oxidative chain reactions that cause cellular damage [27]. Solvent selection critically influences phenolic extraction efficiency due to the polarity-dependent solubility of these compounds. While water, methanol, ethanol, acetone, and chloroform are commonly employed extraction solvents, organic solvents present limitations for phytochemical applications due to their inherent cytotoxicity [7]. The comparative analysis revealed water's superior performance, extracting approximately twice the phenolic content from *O. vulgare* leaves compared to methanol (Table 1). This enhanced yield stems from water's higher polarity, which preferentially solubilizes polar antioxidant compounds. Notably, while methanol demonstrates greater efficacy in disrupting non-polar cell wall components to liberate bound polyphenols [28], its cytotoxic nature renders aqueous extracts more suitable for therapeutic applications. This polarity-extractability relationship underscores the importance of solvent selection in balancing extraction efficiency with biocompatibility for pharmacological uses.

The systematic investigation of extraction parameters (solvent type, duration, temperature) revealed that temperature exerted the most significant effect on extraction yield and phenolic compound concentration from *O. vulgare* leaves, achieving optimal results within 15 min. Elevated temperatures facilitate cell wall disruption, thereby enhancing phenolic compound release into the solvent [32]. As summarized in Table 1, we compared the TPC of *O. vulgare* essential oil, extracts, and AgNPs in this study with literature values for *O. vulgare* preparations. Notably, TPC and total flavonoid content (TFC) vary considerably among plants across regions, which is attributable to environmental and genetic factors such as climate, cultivar, geographical location, and extraction methodologies [33]. For instance, Kaurinović et al. [29] reported the following TPC and TFC extraction efficiency sequence for *O. vulgare*: ethyl acetate > water > n-butanol > ether > chloroform. Contrastingly, Lagouri and Alexandri [30] demonstrated higher TPC in aqueous *Origanum dictamnus* extracts compared to methanolic extracts, whereas Amal et al. [34] observed the opposite trend for *O. vulgare* with methanol outperforming acetone and dichloromethane. Similarly, Bendini et al. [35] found ethanol to be more effective than diethyl ether, n-hexane, and n-pentane for TPC and TFC extraction. Alternative methods such as distillation have also been employed for phenolic compound extraction. Kaurinović et al. [29] and Mechergui et al. [31] reported TPC values of 10.29 and 17.61

mg gallic acid/g dry weight for *O. vulgare* aqueous extract and essential oil, respectively. Consistent with these findings, our results (Table 1) indicated that the aqueous extract and corresponding AgNPs exhibited higher TPC and color intensity than their methanolic counterparts. Other studies on the aqueous essential oil extracted from *O. vulgare* grown in the Arid Andean Region of Chile revealed a remarkably high TPC of 102.71 ± 3.87 mg Gallic acid /g sample, significantly exceeding previously documented levels for this species. This elevated phenolic concentration indicates a rich presence of bioactive compounds, likely enhancing the oil's potent antimicrobial activity, as evidenced by its strong efficacy against key pathogenic and foodborne bacteria [36]. Quantitative analysis via Beer's law [37] revealed concentrations of 1.44 and 0.4 nmol/mL for aqueous and methanolic AgNPs, respectively. This concentration-dependent behavior was further corroborated by UV-Vis spectroscopy and SEM analysis, which confirmed the superior concentration of aqueous AgNPs.

Mechanistically, phytochemicals (e.g., polyphenols, terpenoids, phenolic acids, alkaloids, and sugars) in plant extracts serve dual roles as reducing and capping agents, thereby stabilizing AgNPs [38].

Table 1. Comparison of total phenol content of the *O. vulgare* essential oil, extracts, and AgNPs in this study and *O. vulgare* extracts and essential oils in the literature.

Oil essential and Extract/AgNPs	Total phenols content (mg Gallic acid/g)	Reference
Essential oil	12.3 ± 0.3b	Present study
Aqueous	60 ± 1d	Present study
Aqueous AgNPs	8.4 ± 0.1a	Present study
Methanol	28 ± 1c	Present study
Methanolic AgNPs	27.5 ± 1.5c	Present study
Water	10.29 ± 0.04	
Ether	5.02 ± 0.01	
Chloroform	4.72 ± 0.01	Kaurinovic et al [29]
Ethyl acetate	14.13 ± 0.05	
n-butanol	8.27 ± 0.02	
Water	4.0	Lagouri and Alexandra, [30]
Methanol	7.7	
Aqueous	10.3	Kaurinovic et al. [29]
Essential oil	17.7	Mechergui et al. [31]

Each value is presented as the mean ± SD (n = 3). Values in the same column followed by different letters are significantly different at $p < 0.05$.

3.3. DPPH radical scavenging activity

The antioxidant properties of *O. vulgare* extracts and AgNPs were evaluated using the DPPH radical scavenging assay. Methanolic AgNPs demonstrated remarkable antioxidant activity (89.7% ± 0.2), comparable to synthetic BHT (93.0% ± 0.4), while the essential oil showed limited efficacy (26.7% ± 0.6). Interestingly, although the methanolic extract and its corresponding AgNPs contained similar total phenolic contents, the nanoparticles exhibited significantly enhanced radical scavenging capacity. This boost in activity may be attributed to the dual role of phenolic compounds as reducing and capping agents during nanoparticle synthesis, which potentially increases their bioavailability and reactive

surface area [39]. In contrast, the aqueous extract displayed substantially lower antioxidant effects ($p < 0.05$) that could not be explained by phenolic content alone, suggesting solvent-dependent variations in the extraction of specific antioxidant compounds such as flavonoids, terpenes, and phenolic acids. These findings highlight the importance of extraction methodology and nanoparticle synthesis in optimizing the antioxidant potential of plant-derived materials. Although the aqueous extract demonstrated the lowest antioxidant activity, green synthesis of AgNPs using this extract significantly enhanced antioxidant performance, achieving levels comparable to the toxic methanolic extract. The antioxidant efficacy of *O. vulgare* derivatives was further quantified through IC50 determinations, representing the concentration required for 50% DPPH radical scavenging. As shown in Table 2, all tested extracts and AgNPs exhibited potent antioxidant activity, with IC_{50} values ranging from 19.6 ± 0.3 to 59.7 ± 0.9 μg/mL (inverse correlation with activity). Notably, these values compare favorably with other reports on *Origanum* species, as the researchers in [40] reported IC_{50} values of 28–42 μg/mL for methanolic extracts of *O. vulgare* ssp. vulgare, aligning with our findings (19.6–59.7 μg/mL). The superior activity of our AgNPs may stem from enhanced phytochemical bioavailability through nanoparticle conjugation. Sarikurkcu et al. [41] observed that essential oils from *O. vulgare* subspecies showed IC_{50} values between 45–160 μg/mL, which were substantially higher than our essential oil (59.7 μg/mL), suggesting geographic or varietal influences on antioxidant potential. Drying methods studied by Ozdemir et al. [42] affected IC_{50} values by 20-35%, highlighting processing as a critical factor in activity retention; a consideration for future extraction optimization. These comparative analyses demonstrate that *O. vulgare* from Northwest Iran exhibits competitive antioxidant properties, with AgNP synthesis offering a promising strategy for activity enhancement. The inverse IC_{50}-activity relationship was consistently observed, validating our methodology against international benchmarks.

The literature demonstrates significant variability in the DPPH radical-scavenging capacity of plant extracts, with solvent polarity playing a decisive role. As reported by Exarchou et al. [43], ethanol extracts consistently outperform acetone extracts, while Kaurinović et al. [29] documented superior activity in polar fractions (water and *n*-butanol; IC_{50} = 12.9 μg/mL) compared to chloroform (IC_{50} = 19.9 μg/mL) for *O. vulgare* L. from Serbia. Similarly, Şahin et al. [16] established methanol as more effective than essential oils, a finding corroborated by studies on *O. vulgare* subsp. glandulosum (IC_{50}: 59.2–79.8 μg/mL) [31]. In alignment with these trends, this study revealed that biosynthesized AgNPs exhibited enhanced antioxidant activity relative to their parent extracts, a phenomenon well-documented in nanobiotechnology literature. For instance, *Bergenia ciliata* AgNPs showed 59.3% scavenging versus 51.3% for the methanolic extract [44], and *Chenopodium murale* nanoparticles achieved 65.4 ± 0.2% compared to 59.4 ± 0.1% for the aqueous extract [45]. Notably, Ajayi and Afolayan [46] reported AgNPs of *Cymbopogon citratus* with 70.1% activity (IC_{50}: 30.6 μg/mL), underscoring the consistent efficacy of phytosynthesized nanoparticles. The obtained results confirm that methanolic and aqueous extracts of *O. vulgare* L. serve as optimal media for AgNPs biosynthesis, yielding nanoparticles with clinically relevant antioxidant potential for degenerative disease and oncotherapy applications.

Table 2. Comparison of DPPH radical scavenging activities and IC50 (μg/cm^3) values of the *O. vulgare* extracts and AgNPs in this study and some biosynthesized AgNPs, *O. vulgare extracts*, and essential oils in the literature.

Essential oil and Extract/Ag NPs	DPPH (% scavenging)	IC_{50} (μg/mL)	Reference
Essential oil	29.7 ± 0.6a	59.7 ± 0.9d	Present study
Aqueous	66.2 ± 1.0b	29.1 ± 1.3c	Present study
Aqueous Ag NPS	84.9 ± 0.5c	24.4 ± 1.4b	Present study
Methanol	86.9 ± 2.3c	24.5 ± 0.9b	Present study
Methanolic Ag NPS	89.7 ± 0.2d	19.6 ± 0.4b	Present study
BHT	93.0 ± 0.4de	0.15 ± 0.01a	
Water		11.2	
Ether		23.8	
Chloroform		19.9	Kaurinovic et al. [29]
Ethylacetate		14.1	
n-Butanol		12.9	
Ethanol	95.8		Exarchou et al. [43]
Acetone	33		
Methanol		9.9 ± 0.5	Sahin et al. [16]
Essential oil		89.0 ± 5.0	
Essential oil	57.2 ± 1.6		Sarikurkcu et al. [41]
	32.7 ± 0.9		Ozdemir et al. [42]
Essential oil of 3 populations of *O. vulgari* subsp. Glandulosum	59.2		
Nefza	60.8		Mechergui et al. [31]
Bargou	79.8		
Krib			
Methanol (*Bergenia ciliata*)	59.4 ± 0.1		Phull et al. [44]
Ag NPS *(Bergenia ciliata)*	65.4 ± 0.2		
Aqueous *(Chenopodium murale)*	59.4 ± 0.1		Abdel-Aziz et al. [45]
Ag NPS *(Chenopodium murale)*	65.4 ± 0.2		
AgNPs (*Cymbopogon citratus*)	70.1	30.60	Ajayi and Afolayan, [46]

Each value is presented as the mean ± SD (n = 3). Values in the same column followed by different letters are significantly different at $p < 0.05$.

3.4. Antifungal tests

The essential oil of *O. vulgare* demonstrated dose-dependent antifungal activity against *A. niger*, *Botrytis cinerea*, and *P. expansum* in PDA culture assays. Fungal colony diameters exhibited an inverse relationship with essential oil concentration, with maximal growth inhibition observed at 800-1000 mg/L treatments. Complete suppression of all three fungal species (100% inhibition) was achieved at the highest concentration tested (1000 mg/L), evidenced by the absence of visible colony formation (Figure 3). The oil exhibited broad-spectrum efficacy, with most treatments exceeding 50% inhibition. Notably, *A. niger* displayed the highest resistance among tested species, showing the

weakest response (lowest inhibition percentage) at the minimal concentration of 200 mg/L. Studies have demonstrated that oregano oil exhibits strong antibacterial activity against pathogenic and phytopathogenic bacteria. Notably, *Staphylococcus aureus*, *Salmonella enterica*, *Erwinia rhapontici*, and *Xanthomonas campestris* were found to be the most susceptible, requiring minimal concentrations of the oil to inhibit their growth. Additionally, oregano oil was effective against bacteria linked to foodborne illnesses, highlighting its potential as a natural antimicrobial agent [36].

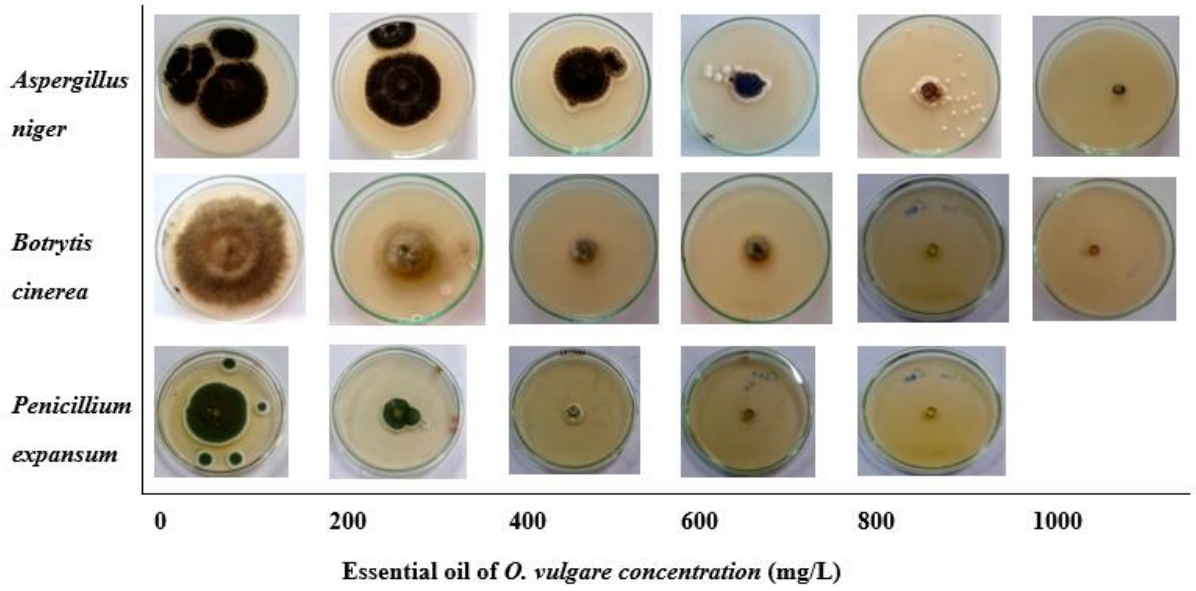

Figure 3. Inhibition effect of essential oil of *O. vulgare* against *Aspergillus niger, Botrytis cinerea*, and *Penicillium expansum* on PDA *in vitro*. In all three fungal species examined, the growth rate declined progressively with increasing concentrations of the essential oil. Notably, the growth of *P. expansum* was inhibited at concentrations of 600 mg/L and above, while *Aspergillus* spp. required a higher concentration of 1000 mg/L for complete growth suppression.

All tested extracts and AgNPs exhibited inhibitory activity against the target fungal strains; however, the AgNPs demonstrated significantly stronger antifungal effects compared to the crude extracts (Figure 4). As illustrated in Figure 5, methanolic AgNPs displayed the highest antifungal efficacy, achieving 51 ± 1% inhibition against *P. expansum*, whereas the aqueous extract showed the lowest activity (10.8 ± 0.7% inhibition) against *A. niger*. Statistical analysis confirmed a significant difference ($p < 0.05$) in the percentage inhibition zones between the extracts and AgNPs. Notably, the use of methanolic AgNPs enhanced antifungal activity by more than twofold compared to the crude extracts, underscoring their superior potential for fungal control applications.

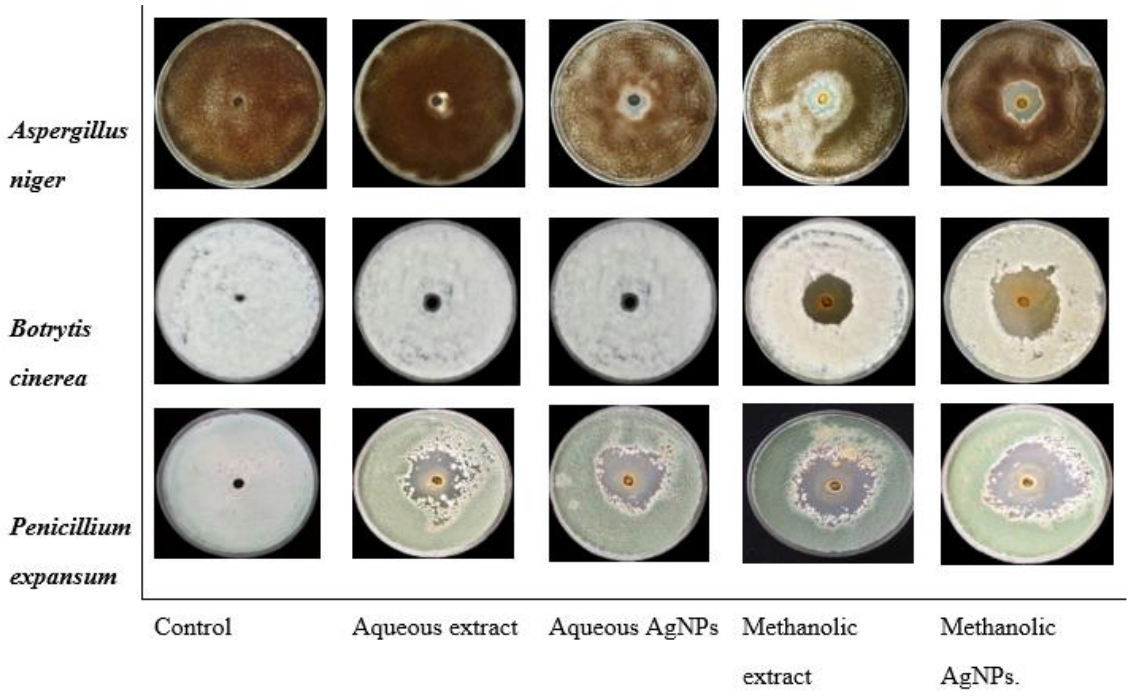

Figure 4. Inhibition effect of extracts/Ag NPs of *O. vulgare* against *Aspergillus niger*, *Botrytis cinerea*, and *Penicillium expansum* on PDA *in vitro*. In all three fungal species tested, the methanol extract and methanolic $AgNO_3$ solution yielded the largest growth inhibition zones, indicating their superior antimicrobial efficacy. Notably, in *Penicillium* spp., the aqueous extract and aqueous $AgNO_3$ also demonstrated significant inhibitory effects, with zone diameters exceeding those observed in the other fungi.

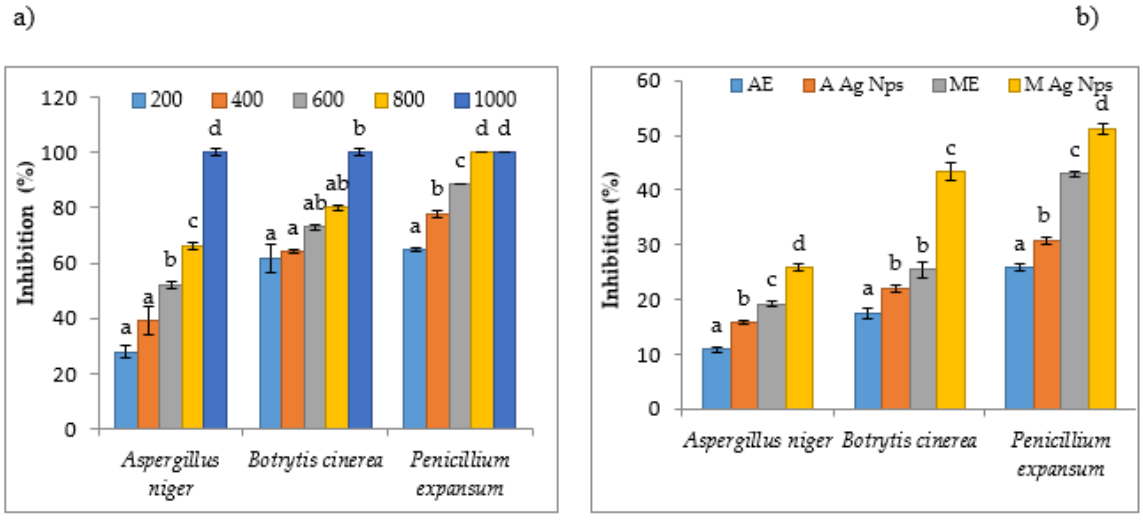

Figure 5. Inhibition (%) of a) essential oil and b) extracts/AgNPs of *O. vulgare* against *Aspergillus niger*, *Botrytis cinerea*, and *Penicillium expansum*. The column represents the mean value ±SD (n = 3), vertical bars show standard deviation, and different letters imply significant differences at $p < 0.05$.

The enhanced antifungal efficacy of methanolic AgNPs compared to their aqueous counterparts stems from their superior cellular penetration capability, attributable to their smaller particle size (18.35 ± 0.9 nm vs 19.43 ± 1.2 nm). Similarly, green-synthesized AgNPs using *Aloe vera* extract demonstrated potent dose-dependent antifungal activity, with inhibition zones ranging from 10 mm to 22 mm against *Candida albicans* ATCC 10231 [47]. It has been reported that ZnO nanoparticles (ZnO-NPs) synthesized using the *Thymus syriacus* plant extract exhibit strong antibacterial activity against Gram-positive and Gram-negative bacterial species [16]. Hashem et al. [48] demonstrated that biosynthesized AgNPs have significant antifungal properties against all fungal strains evaluated. The AgNPs effectively inhibit the growth of *A. niger*, *Aspergillus terreus*, *Aspergillus flavus*, and *Aspergillus fumigatus* at a concentration of 500 μg/mL, resulting in inhibition zones measuring 16 mm, 20 mm, 26 mm, and 19 mm, respectively [48]. AgNPs in solution have the potential to attach to, and saturate, fungal hyphae, leading to the destruction of fungal cells. This inhibitory action is largely due to the presence of Ag+, which primarily impacts the activity of membrane-associated enzymes, particularly those involved in the respiratory chain. Furthermore, AgNPs can engage with substrates via a mechanism called competitive inhibition, which inactivates enzymes and hinders the synthesis of essential products necessary for cellular functions [48]. These nanoparticles exert their fungicidal effects through multiple mechanisms: (1) Binding to membrane proteins and lipids to disrupt structural integrity, (2) interaction with intracellular biomolecules including DNA, and (3) induction of oxidative stress [49]. This multifactorial action is augmented by phytochemical capping agents, particularly phenolic compounds and tannins identified in *O. vulgare* extracts, which synergistically modulate fungal growth and metabolism [14].

GC-MS analysis revealed four dominant bioactive constituents responsible for nanoparticle stabilization and antimicrobial activity: carvacrol (42.7%), thymol (18.3%), γ-terpinene (12.1%), and *p*-cymene (9.8%) [14,50]. These compounds demonstrate well-documented mechanisms: Carvacrol disrupts membrane potential, thymol inhibits ergosterol biosynthesis, and terpenes interfere with mitochondrial function. The therapeutic potential of these phytochemicals extends beyond antifungal applications, as evidenced by their broad-spectrum biological activities, including antimicrobial, anti-inflammatory, and anticancer properties (Table 3).

Extensive research has demonstrated that essential oils containing high concentrations of carvacrol, thymol, and p-cymene exhibit strong antifungal activity against *Candida* spp., *Candida albicans*, *Cryptococcus neoformans*, *Aspergillus* spp., and *Botrytis cinerea* [50–53]; however, their practical application is limited by volatility, oxidative instability, and low extraction yields, necessitating large quantities of plant material [54]. To address these challenges, we synthesized stable and low-toxicity AgNPs, which demonstrated superior antifungal activity at significantly lower concentrations; methanolic AgNPs (0.4 nmol/L) and aqueous AgNPs (1.44 nmol/L) compared to essential oils (1000 mg/L). The enhanced efficacy of AgNPs was attributed to their high surface-area-to-volume ratio, facilitating greater interaction with fungal cell walls [49], as well as their resistance to degradation. Among the tested pathogens, *P. expansum* was the most susceptible, with complete inhibition (100% ± 1) achieved using essential oils (800 mg/L), while methanolic AgNPs (51% ± 1) and aqueous AgNPs (30.8% ± 0.7) exhibited potent activity at nanomolar concentrations, demonstrating their potential as next-generation antifungal agents with improved stability and reduced dosage requirements.

Table 3. Comparison of some *O. vulgare* essential oil compositions (%) determined by GC/MS. (RI: Retention index and RT: Retention time).

Compound	RI	R.T.	Composition (%)						
			Present study	Reference					
				Roofchaee et al. (2011) [59]	Sarikurkcu et al. (2015) [41]	Morshedloo et al. (2017) [8]	Ozdemir et al. (2017) [42]	Vazirian et al. (2015) [9]	Grulová et al. (2020) [60]
α-thujen	927	5.1	0.5	0.3	0.4	1.3	1.6	0.4	-
α-pinene	931	5.3	0.3	0.2	0.2	0.8	0.8	0.4	0.2
1-Octen-3-ol	975	6.1	0.4	-	0.4	0.09	-	-	-
β-myrcene	989	6.4	0.8	0.3	-	2.0	2.6	0.6	-
α-Phellandrene	1005	6.6	0.2	-	-	0.01	0.4	-	-
α-terpinene	1015	6.9	1.0	0.8	1.1	1.2	2.7	1.0	0.70
p-Cymene	1026	7.1	6.2	1.3	13.4	12.0	5.8	3.6	5.7
Limonene	1028	7.2	0.3	0.5	-	0.1	0.3	-	-
γ-terpinene	1060	7.9	5.7	-	4.6	9.7	14.3	9.7	2.5
Trans-sabinene hydrate	1068	8.0	0.3	0.2	-	0.06	-	-	-
Linalool	1099	8.8	0.2	-	-	-	-	0.3	2.6
Borneol	1168	10.4	0.7	0.2	1.0	0.6	0.3	0.06	0.8
Terpineol-4	1180	10.7	0.7	0.8	-	0.1	0.7	0.3	0.7
α-Terpineol	12	11	0.1	0.09	-	0.1	-	1.2	0.4
Carvacrol methyl ether	1245	12.2	2.08	-	-	1	-	6.9	-
Thymol	1295	13.3	21.1	3.3	58.3	3.7	15.5	37.1	76
Carvacrol	1303	13.5	56.5	86.0	16.2	45.9	46.4	9.6	3.2
Trans-caryophyllene	1425	16.2	1.6	1	-	0.5	3.0	1.9	-
β-bisabolen	1509	17.9	0.3	0.4	0.2	0.2	1.2	-	-
Spathulenol		19.3	0.2	-	-	-	-	0.55	-
Caryophyllene oxide	1590	19.2	0.3	-	0.4	0.1	-	0.7	0.4

Researchers have documented the antifungal potential of AgNPs, with varying degrees of efficacy reported across biological systems. Phull et al. [44] observed a maximum inhibition zone of 8 ± 0.57 mm against *A. niger* using *Bergenia ciliata*-derived AgNPs, whereas Jafari et al. [17] reported significantly greater activity (35 mm inhibition zone) for *Thymus vulgaris* L. AgNPs against the same pathogen. Kim et al. [55] demonstrated dose-dependent inhibition of *Botrytis cinerea* (80.7% at 100 mg/L), while Derbalah et al. [56] identified *Euonymus japonicus* extract (90.9% inhibition) and *Bacillus subtilis* culture filtrate (75.6%) as particularly effective against this pathogen. Notably, our study represents the first report of *O. vulgare* L. AgNPs exhibiting enhanced antifungal activity against *P. expansum*, attributable to their nanoscale dimensions and high surface-area-to-volume ratio. In a study, biosynthesized silver nanoparticles using *Polyalthia longifolia* leaf extract (PL-AgNPs) exhibited

strong antifungal activity against *Alternaria alternata*, with a mean particle size of 14 nm and MIC/MFC values reported, highlighting their stability, eco-friendliness, and efficacy as plant-protective agents [57].

Although the precise mechanisms underlying AgNP-mediated antifungal activity remain incompletely understood, evidence suggests a multi-faceted mode of action: (1) Adsorption to cell wall components, compromising structural integrity and increasing membrane permeability; (2) intracellular penetration, leading to organelle dysfunction; and (3) disruption of protein synthesis via enzyme inhibition, suppressing mycelial growth [1,14]. These findings collectively underscore the potential of AgNPs as versatile antifungal agents, with efficacy contingent upon nanoparticle characteristics and target pathogen susceptibility.

3.5. Chemical composition of essential oils by gas chromatography-mass spectrometry (GC-MS)

The essential oil yield of *O. vulgare* was 2.13 ± 0.04% (w/w) of dry matter, with GC/MS analysis (Figure 6) revealing 23 major components representing 99.9% of the total oil composition, dominated by carvacrol (56.5%) and thymol (21.1%), followed by p-cymene (6.2%), γ-terpinene (5.7%), carvacrol methyl ether (2.0%), trans-caryophyllene (1.6%), and α-terpinene (1.0%). Comparative analysis with other geographical variants showed significant chemotypic variation: While we found carvacrol as the major component, other reports demonstrated different profiles; Kordestan, Iran (46% carvacrol, 12% *p*-cymene) [8], Mazandaran, Iran (37.1% thymol, 9.6% carvacrol) [9], Turkey (46.4% carvacrol, 15.5% thymol) [42], and Slovakia (76% thymol, 5.7% *p*-cymene) [41]. These variations likely reflect differences in environmental conditions, growing seasons, and genetic factors that influence secondary metabolite production in this medicinally important species. Simirgiotis et al. [36] discovered fifty metabolites of *O. vulgare* in the Andes region through the use of gas chromatography-mass spectrometry (GC-MS). These metabolites included monoterpene hydrocarbons, oxygenated monoterpenes, phenolic monoterpenes, sesquiterpene hydrocarbons, and oxygenated sesquiterpenes, which were found in the essential oil of oregano sourced from the Atacama Desert. The predominant constituents of the essential oil were thymol (15.9%), *Z*-sabinene hydrate (13.4%), γ-terpinene (10.6%), *p*-cymene (8.6%), linalyl acetate (7.2%), sabinene (6.5%), and carvacrol methyl ether (5.6%) [36]. The observed variations in essential oil composition among geographically distinct populations of *O. vulgare* are primarily attributable to differences in environmental conditions, including climate, soil composition, and altitude, which collectively influence the plant's secondary metabolite production [58].

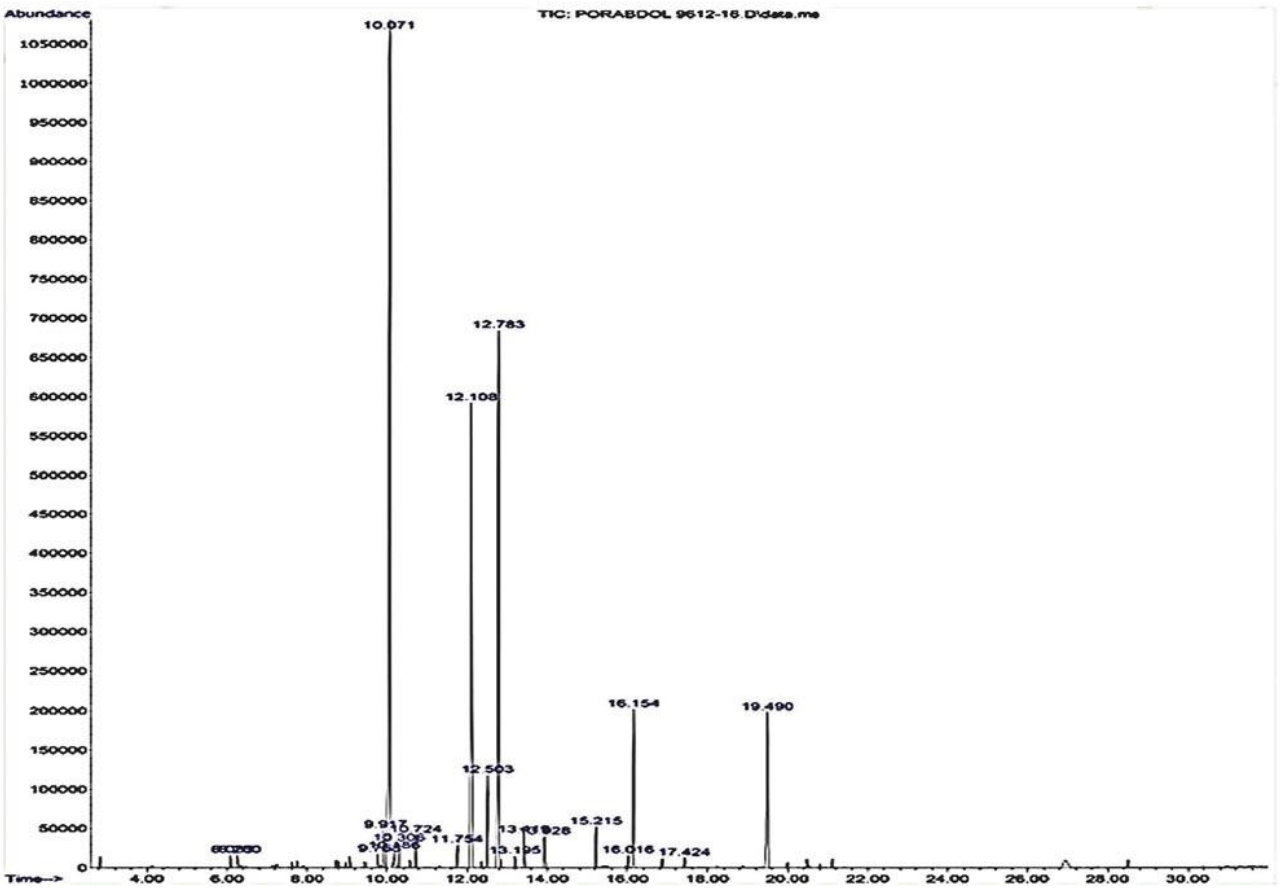

Figure 6. Gas chromatography and mass spectroscopy chromatogram of the essential oils of *O. vulgare* L.

4. Conclusions

In this study, we employed solvent extraction and distillation methods to obtain bioactive compounds from *O. vulgare*, a plant widely used in Iranian cuisine and traditional medicine. The extraction process parameter (solvent type) significantly influenced the yield of bioactive compounds and their antioxidant activity. Notably, while the methanolic extract exhibited lower total phenolic content than the aqueous extract, it demonstrated superior DPPH radical scavenging activity. Green synthesis of AgNPs using *O. vulgare* extracts revealed that phytochemicals in the plant material effectively served as reducing and capping agents, producing stable AgNPs. Antioxidant and antifungal activities (against *A. niger*, *Botrytis cinerea*, and *P. expansum*) were concentration-dependent for the essential oil and inversely correlated with AgNPs size. Methanolic AgNPs, with the smallest particle size, displayed the highest total phenolic content, antioxidant capacity, and antifungal efficacy. Complete fungal inhibition was achieved at essential oil concentrations of 800 and 1 mg/mL. GC-MS analysis identified 23 constituents in the essential oil, with carvacrol (56.53%), thymol (21.18%), *p*-cymene (6.22%), and γ-terpinene (5.67%) as the dominant components. This study suggests that essential oil exhibits significant potential as a natural antifungal agent, while AgNPs demonstrate greater efficacy than plant extracts in controlling plant pathogens. These findings indicate that the tested essential oil, extracts, and AgNPs could serve as readily accessible sources of natural

antioxidants and antifungal compounds for applications in dietary supplements or pharmaceutical formulations.

Use of AI tools declaration

The authors declare they have not used Artificial Intelligence (AI) tools in the creation of this article.

Acknowledgments

This work was conducted in the ambit of the Collaboration Agreement between Prof. Jelena Popović-Djordjević and Prof. Angelo Maria Giuffrè titled: New horizons of production and sustainability for: foods, water, beverages and agricultural products.

Conflict of Interest

The authors declare that there is no conflict of interest regarding the publication of this article. All the authors reviewed the paper and approved the final version.

Author contributions

Conceptualization and supervision: LP; Methodology and writing initial draft: NF; formal analysis, writing- editing and review: SSM; software: J.P.D. and A.M.G.; resources: J.P.D. and A.M.G.; writing—review and editing: J.P.D. and A.M.G.; visualization: J.P.D. and A.M.G.; supervision: J.P.D. and A.M.G.; project administration, J.P.D. and A.M.G.

References

1. Beyrami Miavaghi M, Pourakbar L (2016) Phytosynthesis of silver nanoparticles by medicinal plant Malva neglecta. *Qom Univ Med Sci J* 10: 38–44.
2. Nurani SJ, Saha CK, Khan MAR, et al. (2015) Silver nanoparticles synthesis, properties, applications and future perspectives: A short review. *J Electr Electron Eng* 10: 117–126.
3. Jahan QSA, Sultana Z, Ud-Daula MA, et al. (2024) Optimization of green silver nanoparticles as nanofungicides for management of rice bakanae disease. *Heliyon* 10: e27579. https://doi.org/10.1016/j.heliyon.2024.e27579
4. Shi H, Wen H, Xie S, et al. (2023) Antifungal activity and mechanisms of AgNPs and their combination with azoxystrobin against Magnaporthe oryzae. *Environ Sci: Nano* 10: 2412–2426. https://doi.org/10.1039/D3EN00168G
5. Iravani S, Korbekandi H, Mirmohammadi SV, et al. (2014) Synthesis of silver nanoparticles: chemical, physical and biological methods. *Res Pharm Sci* 9: 385–406.
6. Venugopal R, Liu RH (2012) Phytochemicals in diets for breast cancer prevention: The importance of resveratrol and ursolic acid. *Food Sci Human Wellness* 1: 1–13. https://doi.org/10.1016/j.fshw.2012.12.001

7. Tiwari P, Kaur M, Kaur H (2011) Phytochemical screening and extraction: A review. *Int Pharm Sci* 1: 98–106..
8. Morshedloo MR, Mumivand H, Craker LE, et al. (2018) Chemical composition and antioxidant activity of essential oils in *Origanum vulgare* subsp. *gracile* at different phenological stages and plant parts. *J Food Proc Preserv* 42: e13516. https://doi.org/10.1111/jfpp.13516
9. Vazirian M, Mohammadi M, Farzaei M, et al. (2015) Chemical composition and antioxidant activity of *Origanum vulgare* subsp. *vulgare* essential oil from Iran. *Res J of Pharmacogn* 2: 41–46.
10. Goldsby R, Kindt T, Osborne B, et al. (2003) Immune response to infectious diseases. *Kuby Immunol* 2003: 425–448.
11. Moss M (2008) Fungi, quality and safety issues in fresh fruits and vegetables. *J Appl Microbiol* 104: 1239–1243. https://doi.org/10.1111/j.1365-2672.2007.03705.x
12. Balouiri M, Sadiki M, Ibnsouda SK (2016) Methods for in vitro evaluating antimicrobial activity: A review. *J Pharm Anal* 6: 71–79. https://doi.org/10.1016/j.jpha.2015.11.005
13. Pourakbar L, Moghaddam SS, Enshasy HAE, et al. (2021) Antifungal activity of the extract of a macroalgae, *Gracilariopsis persica*, against four plant pathogenic fungi. *Plants* 10: 1781. https://doi.org/10.3390/plants10091781
14. Moretti MD, Peana AT, Franceschini A, et al. (1998) In vivo activity of *Salvia officinalis* oil against *Botrytis cinerea*. *J Essent Oil Res* 10: 157–160. https://doi.org/10.1080/10412905.1998.9700868
15. Soylu S, Kara M, Türkmen M, et al. (2022) Synergistic effect of *Foeniculum vulgare* essential oil on the antibacterial activities of Ag-and Cu-substituted ZnO nanorods (ZnO-NRs) against food, human and plant pathogenic bacterial disease agents. *Inorg Chem Commun* 146: 110103.
16. Şahin B, Aydin R, Soylu S, et al. (2022) The effect of thymus syriacus plant extract on the main physical and antibacterial activities of ZnO nanoparticles synthesized by SILAR method. *Inorg Chem Commun* 135: 109088. https://doi.org/10.1016/j.inoche.2021.109088
17. Jafari A, Pourakbar L, Farhadi K, et al. (2015) Biological synthesis of silver nanoparticles and evaluation of antibacterial and antifungal properties of silver and copper nanoparticles. *Turk J Biol* 39: 556–561. https://doi.org/10.3906/biy-1406-81
18. Singleton VL, Orthofer R, Lamuela-Raventos RM (1999) Analysis of total phenols and other oxidation substrates and antioxidants by means of folin-ciocalteu reagent. *Methods Enzymol* 299: 152–178. https://doi.org/10.1016/S0076-6879(99)99017-1
19. Cuendet M, Hostettmann K, Potterat O, et al. (1997) Iridoid glucosides with free radical scavenging properties from *Fagraea blumei. Helv Chim Acta* 80: 1144–1152. https://doi.org/10.1002/hlca.19970800411
20. Soylu EM, Kurt Ş, Soylu S (2010) *In vitro* and *in vivo* antifungal activities of the essential oils of various plants against tomato grey mould disease agent *Botrytis cinerea*. *Int J Food Microbiol* 143: 183–189. https://doi.org/10.1016/j.ijfoodmicro.2010.08.015
21. Hosseini N, Salehi Arjmand H, Ghorbanpour M, et al. (2013) Chemical analysis of essential oils from different populations of *Ferulago angulata* subsp. *carduchorum* in Iran. *J Med Plants By-Prod* 2: 69–74.
22. Zielińska A, Skwarek E, Zaleska A, et al. (2009) Preparation of silver nanoparticles with controlled particle size. *Proc Chem* 1: 1560–1566. https://doi.org/10.1016/j.proche.2009.11.004
23. Fafal T, Taştan P, Tüzün B, et al. (2017) Synthesis, characterization and studies on antioxidant activity of silver nanoparticles using *Asphodelus aestivus* Brot. aerial part extract. *S Afr J Bot* 112: 346–353. https://doi.org/10.1016/j.sajb.2017.06.019

24. Rashid MU, Bhuiyan MKH, Quayum ME (2013) Synthesis of silver nano particles (Ag-NPs) and their uses for quantitative analysis of vitamin C tablets. *Dhaka Univ J Pharm Sci* 12: 29–33. https://doi.org/10.3329/dujps.v12i1.16297
25. Muthukrishnan S, Bhakya S, Kumar TS, et al. (2015) Biosynthesis, characterization and antibacterial effect of plant-mediated silver nanoparticles using *Ceropegia thwaitesii*—An endemic species. *Ind Crops Prod* 63: 119–124. https://doi.org/10.1016/j.indcrop.2014.10.022
26. Reddy NJ, Vali DN, Rani M, et al. (2014) Evaluation of antioxidant, antibacterial and cytotoxic effects of green synthesized silver nanoparticles by Piper longum fruit. *Mater Sci Eng C* 34: 115–122. https://doi.org/10.1016/j.msec.2013.08.039
27. Pandey KB, Rizvi SI (2009) Plant polyphenols as dietary antioxidants in human health and disease. *Oxid Med Cell Longevity* 2: 270–278. https://doi.org/10.4161/oxim.2.5.9498
28. Ene-Obong H, Onuoha N, Aburime L, et al. (2018) Chemical composition and antioxidant activities of some indigenous spices consumed in Nigeria. *Food Chem* 238: 58–64. https://doi.org/10.1016/j.foodchem.2016.12.072
29. Kaurinovic B, Popovic M, Vlaisavljevic S, et al. (2011) Antioxidant capacity of *Ocimum basilicum* L. and *Origanum vulgare* L. extracts. *Molecules* 16: 7401–7414. https://doi.org/10.3390/molecules16097401
30. Lagouri V, Alexandri G (2013) Antioxidant properties of greek *O. dictamnus* and *R. officinalis* methanol and aqueous extracts—HPLC determination of phenolic acids. *Int J Food Prop* 16: 549–562. https://doi.org/10.1080/10942912.2010.535185
31. Mechergui K, Coelho JA, Serra MC, et al. (2010) Essential oils of *Origanum vulgare* L. subsp. *glandulosum* (Desf.) Ietswaart from Tunisia: chemical composition and antioxidant activity. *J Sci Food Agric* 90: 1745–1749. https://doi.org/10.1002/jsfa.4011
32. Wang T, He F, Chen G (2014) Improving bioaccessibility and bioavailability of phenolic compounds in cereal grains through processing technologies: A concise review. *J Funct Foods* 7: 101–111. https://doi.org/10.1016/j.jff.2014.01.033
33. Yesiloglu Y, Sit L, Kilic I (2013) In vitro antioxidant activity and total phenolic content of various extracts of *Satureja hortensis* L. collected from Turkey. *Asian J Chem* 25: 8311. https://doi.org/10.14233/ajchem.2013.14731
34. Mohamed AA, Ali SI, Sameeh MY, et al. (2016) Effect of solvents extraction on HPLC profile of phenolic compounds, antioxidant and anticoagulant properties of Origanum vulgare. *Res J Pharm Technol* 9: 2009. https://doi.org/10.5958/0974-360X.2016.00410.8
35. Bendini A, Toschi TG, Lercker G (2002) Antioxidant activity of oregano (*Origanum vulgare* L.) leaves. *Ital J Food Sci* 14: 17–24.
36. Simirgiotis MJ, Burton D, Parra F, et al. (2020) Antioxidant and antibacterial capacities of *Origanum vulgare* L. essential oil from the arid Andean Region of Chile and its chemical characterization by GC-MS. *Metabolites* 10: 414. https://doi.org/10.3390/metabo10100414
37. Paramelle D, Sadovoy A, Gorelik S, et al. (2014) A rapid method to estimate the concentration of citrate capped silver nanoparticles from UV-visible light spectra. *Analyst* 139: 4855–4861. https://doi.org/10.1039/C4AN00978A
38. Kuppusamy P, Yusoff MM, Maniam GP, et al. (2016) Biosynthesis of metallic nanoparticles using plant derivatives and their new avenues in pharmacological applications—An updated report. *Saudi Pharm J* 24: 473–484. https://doi.org/10.1016/j.jsps.2014.11.013

39. Leaves L, Leaves L (2014) Antioxidant activity by DPPH radical scavenging method of ageratum conyzoides. *Am J Ethnomed* 1: 244–249.
40. Şahin F, Güllüce M, Daferera D, et al. (2004) Biological activities of the essential oils and methanol extract of *Origanum vulgare* ssp. *vulgare* in the Eastern Anatolia region of Turkey. *Food Control* 15: 549–557. https://doi.org/10.1016/j.foodcont.2003.08.009
41. Sarikurkcu C, Zengin G, Oskay M, et al. (2015) Composition, antioxidant, antimicrobial and enzyme inhibition activities of two *Origanum vulgare* subspecies (subsp. *vulgare* and subsp. *hirtum*) essential oils. *Ind Crops Prod* 70: 178–184. https://doi.org/10.1016/j.indcrop.2015.03.030
42. Ozdemir N, Ozgen Y, Kiralan M, et al. (2018) Effect of different drying methods on the essential oil yield, composition and antioxidant activity of *Origanum vulgare* L. and *Origanum onites* L. *J Food Meas Charact* 12: 820–825. https://doi.org/10.1007/s11694-017-9696-x
43. Exarchou V, Nenadis N, Tsimidou M, et al. (2002) Antioxidant activities and phenolic composition of extracts from Greek oregano, Greek sage, and summer savory. *J Agric Food Chem* 50: 5294–5299. https://doi.org/10.1021/jf020408a
44. Phull A-R, Abbas Q, Ali A, et al. (2016) Antioxidant, cytotoxic and antimicrobial activities of green synthesized silver nanoparticles from crude extract of *Bergenia ciliata*. *Future J Pharm Sci* 2: 31–36. https://doi.org/10.1016/j.fjps.2016.03.001
45. Abdel-Aziz MS, Shaheen MS, El-Nekeety AA, et al. (2014) Antioxidant and antibacterial activity of silver nanoparticles biosynthesized using *Chenopodium murale* leaf extract. *J Saudi Chem Soc* 18: 356–363. https://doi.org/10.1016/j.jscs.2013.09.011
46. Ajayi E, Afolayan A (2017) Green synthesis, characterization and biological activities of silver nanoparticles from alkalinized *Cymbopogon citratus* Stapf. *Adv Nat Sci: Nanosci Nanotechnol* 8: 015017. https://doi.org/10.1088/2043-6254/aa5cf7
47. Arsène MMJ, Viktorovna PI, Alla M, et al. (2023) Antifungal activity of silver nanoparticles prepared using Aloe vera extract against Candida albicans. *Vet World* 16: 18. https://doi.org/10.14202/vetworld.2023.18-26
48. Hashem AH, Saied E, Amin BH, et al. (2022) Antifungal activity of biosynthesized silver nanoparticles (AgNPs) against aspergilli causing aspergillosis: Ultrastructure study. *J Funct Biomater* 13: 242. https://doi.org/10.3390/jfb13040242
49. Kotzybik K, Gräf V, Kugler L, et al. (2016) Influence of different nanomaterials on growth and mycotoxin production of *Penicillium verrucosum*. *PloS one* 11: e0150855. https://doi.org/10.1371/journal.pone.0150855
50. Vardar-Unlu G, Yağmuroğlu A, Unlu M (2010) Evaluation of in vitro activity of carvacrol against Candida albicans strains. *Nat Prod Res* 24: 1189–1193. https://doi.org/10.1080/14786410903565184
51. Chaillot J, Tebbji F, Remmal A, et al. (2015) The monoterpene carvacrol generates endoplasmic reticulum stress in the pathogenic fungus *Candida albicans*. *Antimicrob Agents Chemother* 59: 4584–4592. https://doi.org/10.1128/AAC.00551-15
52. Kedia A, Prakash B, Mishra PK, et al. (2014) Antifungal and antiaflatoxigenic properties of *Cuminum cyminum* (L.) seed essential oil and its efficacy as a preservative in stored commodities. *Int J Food Microbiol* 168–169: 1–7. https://doi.org/10.1016/j.ijfoodmicro.2013.10.008
53. Zhang J, Ma S, Du S, et al. (2019) Antifungal activity of thymol and carvacrol against postharvest pathogens *Botrytis cinerea*. *J Food Sci Technol* 56: 2611–2620. https://doi.org/10.1007/s13197-019-03747-0

54. Moretti MD, Sanna-Passino G, Demontis S, et al. (2002) Essential oil formulations useful as a new tool for insect pest control. *AAPS PharmSciTech* 3: E13. https://doi.org/10.1208/pt030213
55. Kim SW, Jung JH, Lamsal K, et al. (2012) Antifungal effects of silver nanoparticles (AgNPs) against various plant pathogenic fungi. *Mycobiology* 40: 53–58. https://doi.org/10.5941/MYCO.2012.40.1.053
56. Derbalah AS, Elkot GAE, Hamza AM (2012) Laboratory evaluation of botanical extracts, microbial culture filtrates and silver nanoparticles against Botrytis cinerea. *Ann Microbiol* 62: 1331–1337. https://doi.org/10.1007/s13213-011-0388-1
57. Dashora A, Rathore K, Raj S, et al. (2022) Synthesis of silver nanoparticles employing *Polyalthia longifolia* leaf extract and their *in vitro* antifungal activity against phytopathogen. *Biochem Biophys Rep* 31: 101320. https://doi.org/10.1016/j.bbrep.2022.101320
58. Sá Filho JCFd, Nizio DAdC, Oliveira AMSd, et al. (2022) Geographic location and seasonality affect the chemical composition of essential oils of *Lippia alba* accessions. *Ind Crops Prod* 188: 115602. https://doi.org/10.1016/j.indcrop.2022.115602
59. Roofchaee A, Irani M, Ebrahimzadeh MA, et al. Effect of dietary oregano (*Origanum vulgare* L.) essential oil on growth performance , cecal microflora and serum antioxidant activity of broiler chickens. *Afr J Biotechnol* 10: 6177–6183. https://doi.org/10.4314/ajb.v10i32
60. Gruľová D, Caputo L, Elshafie HS, et al. (2020) Thymol chemotype *Origanum vulgare* L. essential oil as a potential selective bio-based herbicide on monocot plant species. *Molecules* 25: 595. https://doi.org/10.3390/molecules25030595

AIMS Press